

Absence of Nceh1 augments 25-hydroxycholesterol-induced ER stress and apoptosis in macrophages^S

Motohiro Sekiya,^{1,*} Daisuke Yamamuro,^{1,†} Taichi Ohshiro,^{1,†} Akira Honda,[§] Manabu Takahashi,[†] Masayoshi Kumagai,^{*} Kent Sakai,[†] Shuichi Nagashima,[†] Hiroshi Tomoda,^{**} Masaki Igarashi,^{*} Hiroaki Okazaki,^{*} Hiroaki Yagyu,[†] Jun-ichi Osuga,[†] and Shun Ishibashi^{2,†}

Departments of Diabetes and Metabolic Diseases,^{*} University of Tokyo, Tokyo 113-8655, Japan; Division of Endocrinology and Metabolism,[†] Department of Medicine, Jichi Medical University, Tochigi 329-0498, Japan; Joint Research Center,[§] Tokyo Medical University Ibaraki Medical Center, Ibaraki 300-0395, Japan; and Department of Microbial Chemistry,^{**} Graduate School of Pharmaceutical Sciences, Kitasato University, Tokyo 108-8641, Japan

Abstract An excess of cholesterol and/or oxysterols induces apoptosis in macrophages, contributing to the development of advanced atherosclerotic lesions. In foam cells, these sterols are stored in esterified forms, which are hydrolyzed by two enzymes: neutral cholesterol ester hydrolase 1 (*Nceh1*) and hormone-sensitive lipase (*Lipe*). A deficiency in either enzyme leads to accelerated growth of atherosclerotic lesions in mice. However, it is poorly understood how the esterification and hydrolysis of sterols are linked to apoptosis. Remarkably, *Nceh1*-deficient thioglycollate-elicited peritoneal macrophages (TGEMs), but not *Lipe*-deficient TGEMs, were more susceptible to apoptosis induced by oxysterols, particularly 25-hydroxycholesterol (25-HC), and incubation with 25-HC caused massive accumulation of 25-HC ester in the endoplasmic reticulum (ER) due to its defective hydrolysis, thereby activating ER stress signaling such as induction of CCAAT/enhancer-binding protein-homologous protein (CHOP). These changes were nearly reversed by inhibition of ACAT1. **In conclusion, deficiency of *Nceh1* augments 25-HC-induced ER stress and subsequent apoptosis in TGEMs. In addition to reducing the cholesteryl ester content of foam cells, *Nceh1* may protect against the pro-apoptotic effect of oxysterols and modulate the development of atherosclerosis.**—Sekiya, M., D. Yamamuro, T. Ohshiro, A. Honda, M. Takahashi, M. Kumagai, K. Sakai, S. Nagashima, H. Tomoda, M. Igarashi, H. Okazaki, H. Yagyu, J.-i. Osuga, and S. Ishibashi. **Absence of *Nceh1* augments 25-hydroxycholesterol-induced ER stress and apoptosis in macrophages.** *J. Lipid Res.* 2014. 55: 2082–2092.

This work was supported by a grant-in-aid from Research Fellowships of the Japan Society for the Promotion of Science for Young Scientists, a grant-in-aid for Scientific Research from the Ministry of Education and Science, the Program for Promotion of Fundamental Studies in Health Sciences of the National Institute of Biomedical Innovation (NIBIO) and JKA through its promotion funds from KEIRIN RACE, and MEXT-Supported Program for the Strategic Research Foundation at Private Universities 2011–2015 “Cooperative Basic and Clinical Research on Circadian Medicine” from the Ministry of Education, Culture, Sports, Science, and Technology of Japan.

Manuscript received 12 May 2014.

Published, JLR Papers in Press, June 1, 2014
DOI 10.1194/jlr.M050864

Supplementary key words KIAA1363 • arylacetamide deacetylase-like 1 • atherosclerosis • foam cells • acyl-CoA:cholesterol acyltransferase • lipase/hormone-sensitive lipase • oxysterols • reverse cholesterol transport • lipid droplets • apoptosis • neutral cholesterol ester hydrolase 1 • endoplasmic reticulum

Atherosclerotic cardiovascular diseases are the leading cause of mortality in industrialized countries, despite advances in the management of coronary risk factors. Heart attacks arise from the thrombotic occlusion of coronary arteries following the rupture of plaques. Characteristic of these rupture-prone plaques is their lipid-rich nature due to the presence of cholesteryl ester (CE)-laden macrophage foam cells (1).

The hydrolysis of intracellular CE, the initial step of reverse cholesterol transport, is catalyzed by multiple enzymes: neutral cholesterol ester hydrolase 1 (NCEH1) (2), also known as KIAA1363 or arylacetamide deacetylase-like 1 (AADACL1) (3), hormone-sensitive lipase (LIPE) (4), and possibly carboxylesterase 1 (CES1) (5, 6). NCEH1 is a microsomal protein tethered to the endoplasmic reticulum (ER) membrane by its N terminus with the rest of the protein containing the catalytic domain residing in the ER

Abbreviations: acLDL, acetyl-LDL; Bip, immunoglobulin heavy chain-binding protein; CE, cholesteryl ester; CHOP, CCAAT/enhancer-binding protein-homologous protein; ER, endoplasmic reticulum; 25-HC, 25-hydroxycholesterol; 27-HC, 27-hydroxycholesterol; *Hmgcs1*, 3-hydroxy-3-methylglutaryl-CoA synthase 1; 7-KC, 7-ketocholesterol; LD, lipid droplet; LIPE, hormone-sensitive lipase; LPDS, lipoprotein deficient serum; LXR, liver X receptor; NCEH1, neutral cholesterol ester hydrolase 1; PPPA, pyripyropene A; Srebp, sterol regulatory element binding protein; TEM, transmission electron microscopy; TGEM, thioglycollate-elicited peritoneal macrophage; TUNEL, Terminal deoxynucleotidyl transferase-mediated dUTP nick end labeling; Xbp-1, X-box-binding protein 1.

¹M. Sekiya, D. Yamamuro, and T. Ohshiro contributed equally to this work.

²To whom correspondence should be addressed.

e-mail: ishishash@jichi.ac.jp

^SThe online version of this article (available at <http://www.jlr.org>) contains supplementary data in the form of three figures.

lumen (7) and is robustly expressed in macrophages (2). In addition to CE, NCEH1 may catalyze the hydrolysis of 2-acetyl monoalkylglycerol (8) and TG (2). We have recently reported that disruption of *Nceh1* promotes the formation of foam cells and accelerates the development of atherosclerosis in mice lacking either *ApoE* or LDL receptor (*Ldlr*) (9). In humans, NCEH1 plays a more critical role in cholesterol removal from monocyte-derived macrophages (10). Ultimately, however, accumulating evidence has suggested that reverse cholesterol transport is only one of a number of diverse functions of macrophages in atherogenesis (11). Macrophage apoptosis is another important feature of atherosclerosis (12, 13). Interestingly, the metabolism of cholesterol and its metabolites is closely involved in the apoptosis of macrophages. For example, oxysterols such as 25-hydroxycholesterol (25-HC) and 7-ketocholesterol (7-KC) are major bioactive molecules that initiate the apoptosis of macrophages exposed to oxidized LDL (14). Sinensky and his colleagues reported that increased Ca^{2+} influx (15) and subsequent activation of cytosolic phospholipase A2 (cPLA2) (16), as well as increased proteasomal degradation of Akt (17), underlie the oxysterol-induced apoptosis in CHO-K1 and P388D1 cells. They further showed that ACAT mediates the 7-KC-induced apoptosis in P388D1 cells and mouse peritoneal macrophages (18). In contrast to this pro-apoptotic role, Rothblat and Tabas reported that ACAT can serve an anti-apoptotic role by showing inhibition of ACAT causes apoptosis of macrophages after exposure to acetyl-LDL (acLDL) (19, 20). Tabas and colleagues further proposed that ER stress pathways mediate apoptotic signaling in this process (21). Thus, the role of ACAT1 in apoptosis may depend on the sort of sterol, which probably explains the conflicting results concerning the effects of ACAT1's inhibition on atherosclerosis (22, 23). Because NCEH1 counteracts ACAT activity, it is possible that macrophages lacking *Nceh1* are more susceptible to apoptosis, particularly in response to various sterols. These considerations have prompted us to examine the anti-apoptotic role of *Nceh1* in the apoptosis of macrophages.

Herein, we demonstrate that *Nceh1*-deficient macrophages are highly susceptible to apoptosis induced by 25-HC, and the underlying mechanism may involve the activation of ER stress signaling due to accumulation of 25-HC ester in the ER.

MATERIALS AND METHODS

Materials

27-Hydroxycholesterol (27-HC) was purchased from Research Plus (Bayonne, NJ); all other oxysterols and MG-132 were purchased from Sigma (St. Louis, MO). Ca^{2+} -free DMEM medium was purchased from Gibco (Carlsbad, CA). K-604 (24) and CS-505 (25) were provided by Kowa Pharmaceutical, Daiichi Sankyo and Kyoto Pharmaceutical Industries, respectively. Pyripyropene A (PPPA) was purified from a culture broth of the fungus, *Aspergillus fumigatus* FO-1289 (26, 27). Cholesterol [$1-^{14}C$]oleate and [$1-^{14}C$]oleic acid were purchased from Perkin Elmer (Waltham,

MA). 25-HC oleate was synthesized from 25-HC and oleic acid with 1-ethyl-3-(3-dimethylaminopropyl)carbodiimide and 4-dimethylaminopyridine in dichloromethane. After reaction, 25-HC oleate was purified by preparative TLC on silica gel (10:1 hexane:ethyl acetate). Chemical structure was determined by the NMR analysis and MS. 25-HC [$1-^{14}C$]oleate was synthesized from 25-HC and [$1-^{14}C$]oleic acid.

Lipoproteins

acLDL and lipoprotein deficient serum (LPDS) were prepared as described previously (28).

Animals

Mice lacking *Nceh1* (*Nceh1*^{-/-}), *Lipe* (*Lipe*^{-/-}) or both (*Nceh1*^{-/-}; *Lipe*^{-/-}) were generated as described previously (9, 29). Mice used in this study were crossed onto the C57BL/6J background for more than five generations. All experimental procedures and handling of animals were conducted according to our institutional guidelines.

Peritoneal macrophages

Thioglycollate-elicited peritoneal macrophages (TGEMs) were obtained from 8-week-old mice as described (9) and incubated in DMEM containing 10% FCS or 10% LPDS.

Transmission electron microscopy

Cells were fixed in modified Karnovsky's phosphate-buffered (0.1 M) glutaraldehyde (2.5%)-paraformaldehyde (4%) mixture at room temperature for 12 h, postfixed for 2 h in 2% osmium tetroxide in 0.1 M phosphate buffer, dehydrated in ethanol and propylene oxide, and embedded in Epon. The sections were cut and then counterstained with uranyl acetate and lead citrate for transmission electron microscopy (TEM).

Detection of DNA ladder

DNA (0.5 μ g), which was extracted from the cells, was end-labeled with [α -³²P]dCTP by Klenow and subjected to electrophoresis in a 1.5% agarose gel and then transferred to nylon membranes, as described previously (30). Mouse thymocyte apoptotic DNA was used as a control (31).

TUNEL

Terminal deoxynucleotidyl transferase-mediated dUTP nick end labeling (TUNEL) was performed by using a kit (Takara Biomedicals, Tokyo). At least 1,500 cells from five random fields were counted in each individual sample, and the percentage of apoptotic cells was calculated as (TUNEL-positive cells)/(TUNEL-positive cells + surviving TUNEL-negative cells).

Subcellular fractionation

Cells were sonicated in buffer A [20 mM Tris-HCl (pH 7.0), 250 mM sucrose with protease inhibitors], ultracentrifuged at 100,000 *g* for 45 min at 4°C, microsomal pellet was resuspended and re-ultracentrifuged to enhance purity to give a supernatant fraction (cytosol) and a microsomal pellet (22, 23).

TLC

Lipid was extracted from the cytosolic (100 μ g of protein) and microsomal fraction (50 μ g of protein), and was separated by TLC with toluene-ethyl acetate (67:33) as the solvent. Visualization was done with 10% sulfuric acid.

Measurements of oxysterols

Concentrations of oxysterols in subcellular fractions were measured using LC-MS/MS as described (32). After the addition of

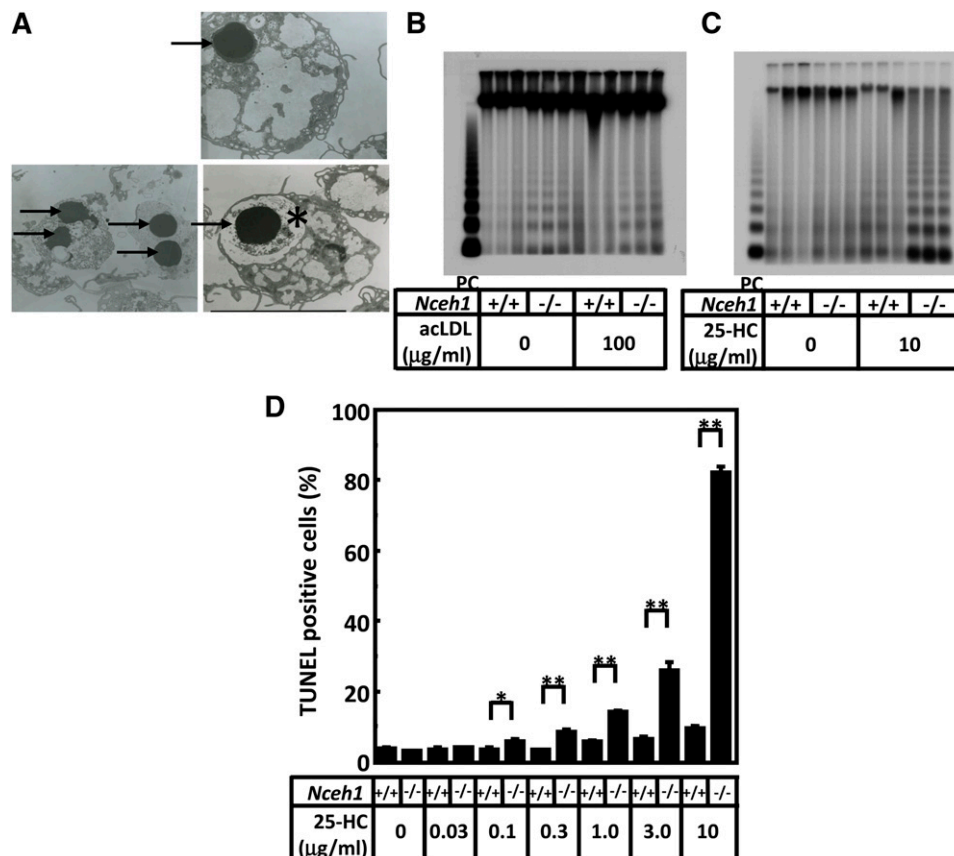


Fig. 1. *Nceh1*-deficient TGEMs are prone to apoptosis. **A:** TEM observation. TGEMs were incubated in DMEM containing 10% FCS. Nuclear condensation (indicated by arrows), a characteristic feature of apoptotic cells, was observed predominantly in *Nceh1*-deficient TGEMs (representative images are shown). *The apoptotic macrophage engulfed by another macrophage. **B, C:** DNA ladder. DNA (0.5 μg) from macrophages was loaded in each lane. PC denotes positive control DNA (0.5 μg) from dexamethasone-treated thymocytes. Three wells of cells were incubated either in DMEM containing 10% FCS with or without acLDL (100 μg/ml) for 24 h (**B**) or in DMEM containing 10% LPDS with vehicle or 25-HC (10 μg/ml) for 24 h (**C**). **D:** Four wells of cells were incubated with increasingly higher concentrations of 25-HC for 24 h. The apoptotic cells were detected by TUNEL. Data are expressed as the mean ± SEM. * $P < 0.05$; ** $P < 0.01$.

deuterated internal standards and butylated hydroxytoluene, each fraction was either hydrolyzed with 1 N ethanolic KOH and derivatized into picolinyl esters, or directly converted into picolinyl esters.

Northern blot analysis

Northern blot analyses were performed as described (9).

Analysis of Xbp-1 mRNA splicing

Total RNA was reverse transcribed and amplified using a sense primer (5'-AAACAGAGTAGCAGCCGAGACTGC-3') and an antisense primer (5'-GGATCTCTAAACTAGAGGCTTGGTG-3'). This fragment was further digested by *PstI* as described previously (33).

Quantitative real-time PCR

Two micrograms of total RNA were reverse-transcribed using the ThermoScript RT-PCR system (Invitrogen). Quantitative real-time PCR was performed using SYBR Green dye (Applied Biosystems, Foster City, CA) in an ABI Prism 7900 PCR instrument (Applied Biosystems). The relative abundance of each transcript was calculated from a standard curve of cycle thresholds for serial dilutions of a cDNA sample and normalized to *Rplp0* or *Atcb*. Primer sequences for *Abca1* and 3-hydroxy-3-methylglutaryl-CoA synthase 1 (*Hmgcs1*) were described previously (9). Other primer sequences were as follows: immunoglobulin heavy chain-binding

protein (*Bip*) (sense 5'-TCATCGGACGCACTTGGAA-3', antisense 5'-CAACCACCTTGAATGGCAAGA-3'), CCAAT/enhancer-binding protein-homologous protein (*Chop*) (sense 5'-GTCCCTAGCTTGCTGACAGA-3', antisense 5'-TGGAGAGCGAGGGCTTTG-3'), *Nceh1* (sense 5'-AGCCTGCAGTTTTCAGCTTA-3', antisense 5'-AGAGTCCGTTATTTCTGGAGACG-3'), *Acat1* (sense 5'-GGAAGTTGGGTGCCACTTCG-3', antisense 5'-GGTGCTCTCAGATCTTTGG-3'), *Rplp0* (sense 5'-GAAGACAGGGCCACCTGGAA-3', antisense 5'-TTGTGGTCCCACAATGAAGC-3'), and *Atcb* (sense 5'-CGATGCCCTGAGGCTCTTT-3', antisense 5'-TGGATGCCACAGGATTCCA-3').

Western blot analyses

TGEMs were homogenized in buffer A [50 mM Tris-HCl, 250 mM sucrose, 1 mM EDTA, 2 μg/ml leupeptin (pH 7.0)]. Ten micrograms of proteins of whole lysates were separated by SDS-PAGE on the NuPAGE 10% Bis-Tris gel and transferred to a nitrocellulose membrane. For detection of the proteins, the membranes were incubated with each anti-murine Akt (Abcam) or anti-murine GAPDH at a dilution of 1:1,000 in Hikari A solution (Nacalai Tesque). Specifically bound immunoglobulins were detected in a second reaction with a horseradish peroxidase-labeled IgG conjugate and visualized by ECL detection (GE Healthcare) with Image Quant LAS 4000 Mini (GE Healthcare).

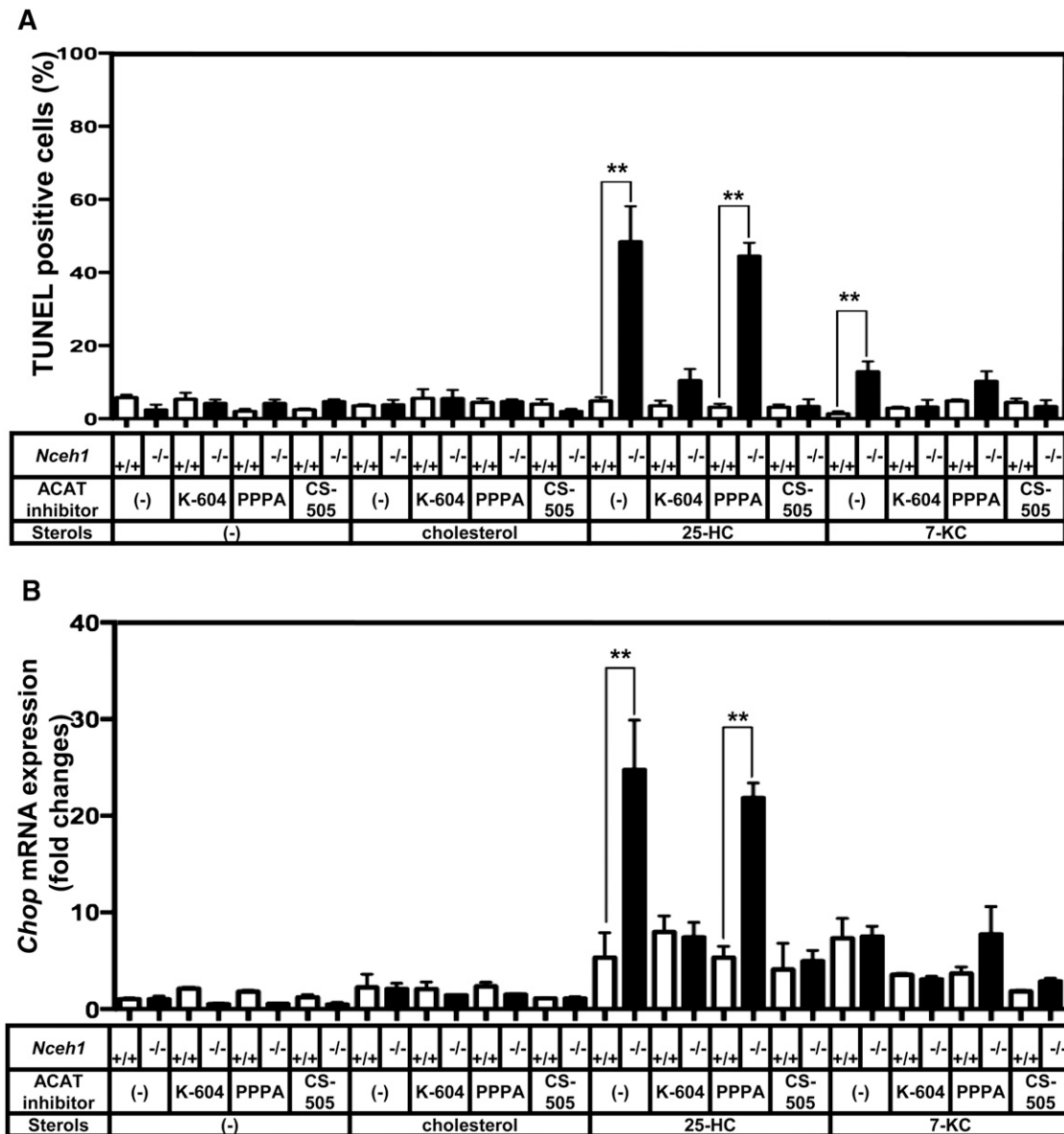


Fig. 2. Inhibition of ACAT1 suppresses the augmentation of 25-HC-induced apoptosis in *Nceh1*-deficient TGEMs. Four wells of TGEMs were incubated in DMEM containing 10% LPDS with vehicle or 25-HC (10 $\mu\text{g}/\text{ml}$) in the presence or absence of the ACAT inhibitors: K-604, PPPA, and CS-505 (10 μM) for 24 h. A: The apoptotic cells were detected by TUNEL. B: Expression of *Chop* was measured by RT-PCR. Data are expressed as the mean \pm SEM. ** $P < 0.01$; NS, a nonsignificant difference.

Statistics

Statistical differences between groups were analyzed by one-way ANOVA and the post hoc Tukey-Kramer test or two-tailed Student's *t*-test, unless otherwise stated.

RESULTS

Nceh1 deficiency increases the susceptibility of macrophages to apoptosis

While attempting to examine the intracellular structures of the *Nceh1*^{-/-} TGEMs using TEM, we noticed a small number of apoptotic cells featuring condensed nuclei in *Nceh1*^{-/-} TGEMs (Fig. 1A). Interestingly, while cellular cholesterol loading with aLDL did not alter the frequency of apoptotic nuclei (Fig. 1B), treatment of *Nceh1*-deficient

TGEMs with 25-HC (Fig. 1C, D; Fig. 2A), 7-KC (Fig. 2A), and 27-HC (data not shown) augmented apoptosis. The *Nceh1*-dependent augmentation of apoptosis was not observed for other compounds including lipopolysaccharide, tunicamycin, staurosporin, 5 α 6 α -epoxycholesterol, 5 β 6 β -epoxycholesterol, 7 β -hydroxycholesterol, and 24-hydroxycholesterol (data not shown). The effects were far more pronounced for 25-HC than for 7-KC and 27-HC, and detectable even at a concentration of 0.1 $\mu\text{g}/\text{ml}$ (0.26 μM) (Fig. 1D), which is close to a physiological concentration of oxysterols (0.01–0.1 μM in plasma) (34).

The augmentation of the 25-HC-induced apoptosis, which was clearly observed in *Nceh1*^{-/-} TGEMs, was not detectable in nonelicited macrophages; treatment with 25-HC significantly increased the number of apoptotic cells as well as the expression of *Chop*, even in nonelicited WT

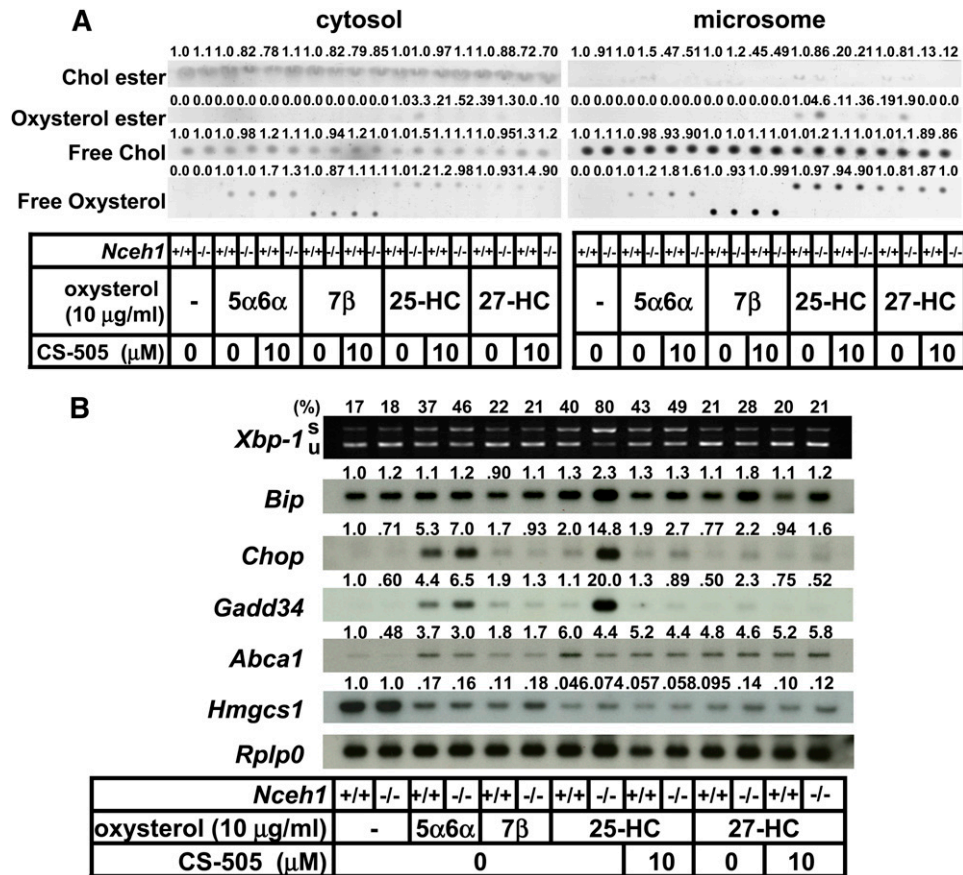


Fig. 4. 25-HC is a highly specific trigger for accumulation of esterified oxysterol and activation of ER stress in *Nceh1*-deficient TGEMs. A, B: TGEMs were incubated with various kinds of oxysterols (10 µg/ml) in the presence or absence of CS-505 (10 µM) for 12 h. Lipids were separated by thin layer chromatography (A), and the expression profile was examined (B). s, spliced; u, unspliced; Chol, cholesterol. Oxysterols are abbreviated as follows: 5α6α, 5α6α-epoxycholesterol; 7β, 7β-hydroxycholesterol. Values above each band/spot indicate the fold difference evaluated by densitometry. Xbp-1 splicing was assessed as the percent spliced Xbp-1 [spliced Xbp-1/(spliced Xbp-1 plus unspliced Xbp-1)].

to remain relatively constant (Fig. 3A). A small amount of 25-HC ester was detected after 1 h of incubation mainly in the microsomal fraction of *Nceh1*^{-/-} TGEMs, and thereafter the intracellular 25-HC ester content increased gradually in *Nceh1*^{-/-} TGEMs. 25-HC ester was not detectable in cells coincubated with CS-505.

The isolated microsomal fraction contains the ER, where *Nceh1* resides, and changes in ER lipid composition are known to initiate ER stress (13, 37). The prolonged activation of ER stress signaling is also known to lead to apoptotic cell death (38). Therefore, we examined whether ER stress mediates the 25-HC-induced apoptosis in *Nceh1*^{-/-} TGEMs. Indeed, the accumulation of 25-HC ester preceded increased expression of ER stress markers such as Chop, Bip, and the spliced form of X-box-binding protein 1 (Xbp-1) (Fig. 3B). Oxysterols inhibit the processing of sterol regulatory element binding protein (Srebp)-2 by binding to an anchor protein called insulin induced genes (Insigs), and block cholesterol biosynthesis (39). Indeed, oxysterols decreased the gene expression of an enzyme involved in cholesterol biosynthesis, *Hmgcs1*, though the expression was not affected by the *Nceh1* genotype. The induction of the *Chop* expression was inhibited

by K-604 and CS-505, but not by PPPA (Fig. 2B). These results further indicate that ACAT1 mediates the augmentation of the 25-HC-induced ER stress. A similar phenomenon was observed for 7-KC.

The augmentation of ER stress signaling in *Nceh1* deficiency was observed specifically for 25-HC, because there was no such robust induction of ER stress for other oxysterols (Fig. 4).

We also investigated whether the cholesterol biosynthetic pathway is involved in the apoptotic process using the HMG-CoA reductase inhibitor, simvastatin. Simvastatin treatment increased macrophage apoptosis as reported previously (40), but this was not influenced by the presence or absence of *Nceh1* (Fig. 5). Furthermore, we investigated the potential contribution of a nuclear oxysterol receptor, liver X receptor (LXR), which regulates cholesterol homeostasis (41). Although a representative target of LXR, *Abca1*, was upregulated by oxysterols, the levels did not correlate with the frequency of apoptosis (Fig. 3B, Fig. 4B).

To test whether the pathways proposed by Sinensky et al. for oxysterol-induced apoptosis are involved in the *Nceh1*-dependent augmentation of 25-HC-induced apoptosis

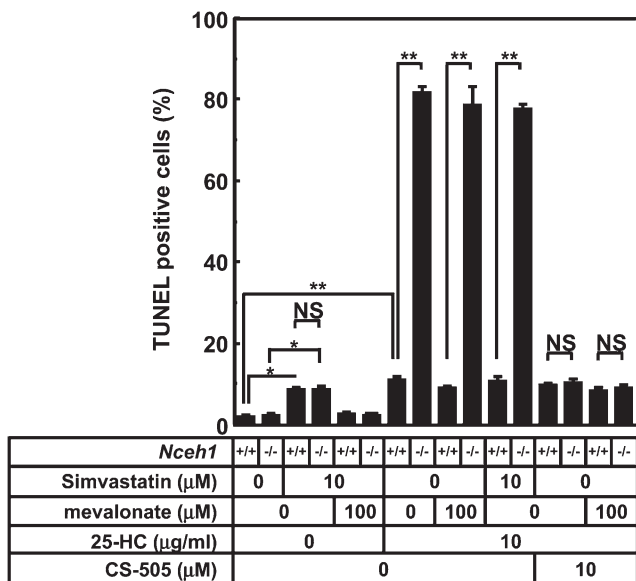


Fig. 5. The evaluation of the contribution of cholesterol biosynthetic pathway. Four wells of TGEMs were incubated in DMEM containing 10% LPDS with compound(s) indicated below the graph for 24 h, and the apoptotic cells were detected by TUNEL method. Data are expressed as the mean \pm SEM. * $P < 0.05$ and ** $P < 0.01$, as determined by ANOVA followed by the Tukey-Kramer post hoc test. NS, nonsignificant difference.

(15–17), we examined the role of Ca^{2+} in the medium in this phenomenon. Elimination of Ca^{2+} from the medium significantly suppressed the 25-HC-mediated apoptosis in WT macrophages, but it did not affect *Nceh1*-dependent augmentation of 25-HC-induced apoptosis (supplementary Fig. IIIA). Next, we examined the effects of 25-HC on Akt degradation. In WT TGEMs, 25-HC decreased the expression of Akt as expected, although we failed to demonstrate that MG-132, a proteasome inhibitor, protects against the 25-HC-dependent degradation of Akt protein. Deletion of *Nceh1* did not further decrease the expression of Akt (supplementary Fig. IIIB). Therefore, it is unlikely that either increased influx of Ca^{2+} or increased degradation of Akt is responsible for the *Nceh1*-dependent augmentation of 25-HC-induced ER stress and subsequent apoptosis.

Lipe is not involved in 25-HC-induced augmentation of macrophage apoptosis

We have previously demonstrated that Lipe also plays a crucial role in the hydrolysis of cholesterol ester in macrophages, although the potential impact of Lipe on foam cell formation and atherogenesis is less than that of *Nceh1* (9). However, the deficiency of Lipe did not affect either the extent of 25-HC-induced apoptosis or the expression of ER stress response markers (Fig. 6A, C). Consistent with the findings, 25-HC ester did not accumulate in *Lipe*^{-/-} TGEMs (Fig. 6B).

Finally, we used LC-MS/MS to measure 25-HC and its esterified form more quantitatively in the TGEMs treated with 25-HC (Fig. 7). 25-HC ester contents were profoundly increased in both microsomal (Fig. 7A) and cytosolic (Fig. 7B)

fractions of *Nceh1*^{-/-} and *Nceh1*^{-/-};*Lipe*^{-/-} TGEMs. Free 25-HC contents were also significantly increased only in the cytosolic fraction of *Nceh1*^{-/-} and *Nceh1*^{-/-};*Lipe*^{-/-} TGEMs (Fig. 7D). There were no significant differences in the free 25-HC contents of microsomal fractions in the cells treated with exogenous 25-HC (Fig. 7C).

DISCUSSION

In the present study, we show that deletion of *Nceh1* makes TGEMs susceptible to 25-HC-induced apoptosis. Because the increased oxysterol-induced apoptosis was nearly reversed by inhibition of ACAT1, we would ascribe this phenomenon to the defective hydrolysis of esterified oxysterols. The mRNA expression of the target molecules of ER stress signals correlated with the apoptosis-inducing capacity of oxysterols and preceded the occurrence of apoptosis. Moreover, the augmented ER stress was associated with the accumulation of 25-HC ester in the ER, both of which were suppressed by inhibition of ACAT1. These results indicate that the oxysterol-induced apoptosis in *Nceh1*-deficient TGEMs is mediated by ER stress provoked by the accumulation of esterified oxysterols in the ER.

Oxysterols are present in atherosclerotic plaques and may play diverse roles in plaque development (42). Oxysterols profoundly affect cholesterol homeostasis. For example, 25-HC potently inhibits cholesterol biosynthesis and is cytotoxic (43, 44). This property has been utilized to isolate mutant cells which are defective in the molecular pathway mediating the sterol-mediated feedback inhibition of cholesterol biosynthesis (45). Subsequent works have identified molecular defects of these mutant CHO cells, not only in SREBP-2 (46, 47) and SREBP cleavage-activating protein (48), but also in ACAT (49, 50). In addition to defective feedback repression of cholesterol biosynthesis, absence of ACAT may be advantageous to antagonize certain toxic effects of 25-HC through a pathway distinct from 25-HC-mediated suppression of cholesterol biosynthesis. Indeed, Freeman et al. (18) showed that ACAT mediates oxysterol-induced apoptosis in macrophages, which is largely consistent with our findings that the *Nceh1*-dependent augmentation of 25-HC-induced ER stress and apoptosis were abrogated by ACAT1 inhibition (Fig. 2).

Given the pro-apoptotic role of ACAT discussed above, it is quite logical that the deficiency in NCEH1, an enzyme mediating a counteraction against ACAT, plays an anti-apoptotic role as we demonstrate herein. It is noteworthy that 25-HC was extremely potent in inducing apoptosis in *Nceh1*^{-/-} TGEMs (Fig. 1D). The increases in the amounts of esterified forms of these oxysterols in the ER appear to be proportional to the apoptotic death (Fig. 3). As 25-HC stimulated ACAT activity in fibroblasts (43) as well as in a cell-free system (51), it is plausible that 25-HC ester is most easily accumulated in cells that lack hydrolyzing activity toward 25-HC ester. Indeed, *Nceh1* hydrolyzes 25-HC ester in vitro (supplementary Fig. II). In this context, it is reasonable that the catalytic domain of *Nceh1* resides in the

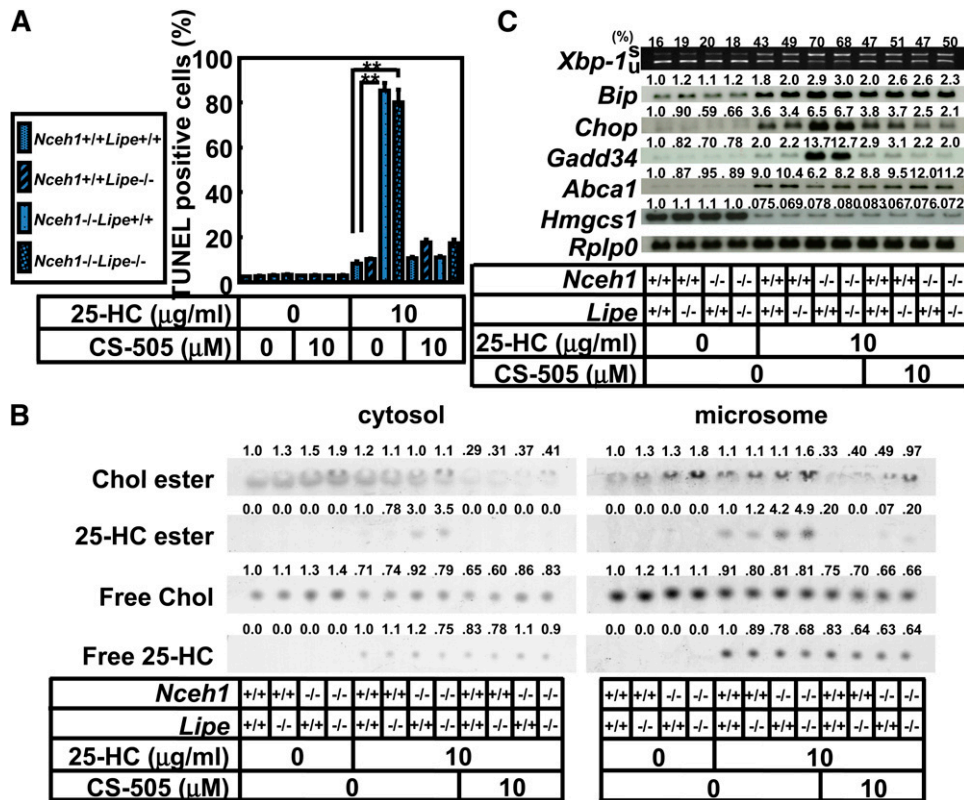


Fig. 6. Lipe is not involved in *Nceh1*-dependent augmentation of 25-HC-induced apoptosis. TGEMs of each genotype (the symbol corresponding to each genotype is given in the inset, four dishes) were incubated with 25-HC (10 μg/ml) in the presence or absence of CS-505 (10 μM) for 24 h, and the apoptotic cells were detected by the TUNEL method. Data are expressed as the mean ± SEM. ***P* < 0.01. B: Lipid separation by TLC. C: Expression profile of ER stress markers. Cells were incubated with 25-HC (10 μg/ml) in the presence or absence of CS-505 (10 μM) for 12 h. s, spliced; u, unspliced; Chol, cholesterol. Values above each band/spot indicate the fold difference evaluated by densitometry. Xbp-1 splicing was assessed as the percent spliced Xbp-1/[spliced Xbp-1/(spliced Xbp-1 plus unspliced Xbp-1)].

ER lumen (7), where the majority of 25-HC ester accumulates (52). The increased amounts of oxysterol esters in the ER may trigger apoptotic signals. In addition to efficient esterification of 25-HC as mentioned above, other chemical properties of 25-HC which are not shared with other oxysterols might account for the susceptibility to this specific oxysterol. The esterified form of 25-HC might be the most potent inducer of ER stress. Probably, hydroxyl moiety at C25 is important for localization in the ER whereby triggering ER stress.

25-HC ester also significantly accumulated in the cytosolic fraction of TGEMs lacking *Nceh1* (Fig. 7B). The newly synthesized 25-HC ester in the microsome might be readily transported to and stored in lipid droplets (LDs). Interestingly, *Lipe* deficiency did not further increase 25-HC ester in the cytosol. Given that 25-HC ester can be hydrolyzed by Lipe in vitro (supplementary Fig. II), LDs containing an excess of 25-HC ester might have an inhibitory effect on the efficient hydrolysis of 25-HC ester by Lipe. In the cytosol, free 25-HC was also increased in TGEMs lacking *Nceh1* (Fig. 7D). We assume that enlarged LDs have large surface area that can accommodate a large amount of free 25-HC.

It is plausible that ER stress mediates apoptotic signaling in the 25-HC-treated *Nceh1*^{-/-} TGEMs. The mRNA

levels of Xbp-1(s), Bip, Chop, and Gadd34 were all significantly elevated in *Nceh1*-deficient TGEMs exposed to 25-HC (Fig. 3). Xbp-1(s) is a downstream target of inositol-requiring protein-1 (IRE1), and CHOP and GADD34 are downstream targets of protein kinase RNA-like ER kinase (PERK) signaling (37). BIP is an ER chaperone that prevents activating transcription factor-6 (ATF6) from moving to the Golgi-apparatus. Therefore, we presume that activation of both the IRE1 and PERK arms is necessary for the induction of apoptosis. In this context, Shibata et al. (53) have recently reported that 25-HC triggers integrated stress response via activation of GCN2/eIF2/ATF4 in macrophages. It would be intriguing to know whether the same pathway is activated in the *Nceh1*-dependent augmentation of 25-HC-induced ER stress, although it is beyond the scope of this study.

In our experiments, there was no discernible difference in the expression levels of genes regulating cholesterol homeostasis such as *Abca1* and *Hmgcs1* between the cells with and without *Nceh1*, even though apoptosis is known to be induced either by inhibition of cholesterol biosynthesis (54) or by suppression of cholesterol efflux (55). Furthermore, the *Nceh1*-dependent augmentation of 25-HC-induced apoptosis does not appear to involve increased Ca²⁺ influx or increased degradation of Akt (supplementary Fig. III).

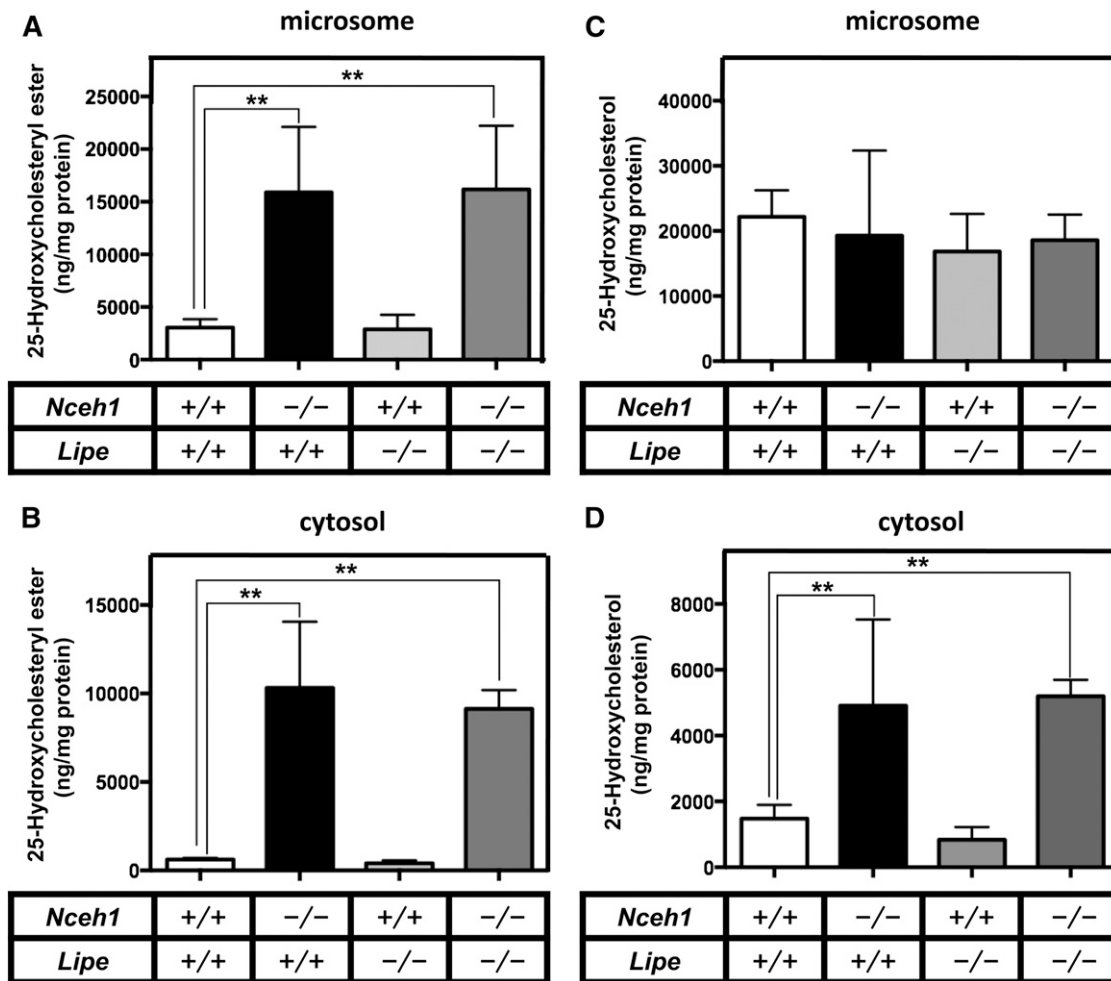


Fig. 7. Quantification of free and esterified 25-HC in subcellular fractions. TGEMs plated at 5×10^6 cells per 6 cm dish in 5–6 dishes were incubated with 10 $\mu\text{g}/\text{ml}$ of 25-HC for 12 h. After cell fractionation, the lipids extracted from the cytosolic (B, D) and microsomal fractions (A, C) were subjected to LC-MS/MS to measure free (C, D) and esterified forms (A, B) of 25-HC. Data are expressed as the mean \pm SEM. ** $P < 0.01$; NS, nonsignificant difference.

As mentioned above, 25-HC is a potent stimulator of ACAT activity (35) and markedly suppresses the SREBP-mediated transactivation of its target genes by binding to Insigs (39). 25-HC also binds other proteins including LXR, cholesterol transporters, and Niemann-Pick C1 (56). In addition to these robust biological effects of 25-HC on cholesterol metabolism, accumulating evidence has suggested that stimulation of Toll-like receptor signaling elicits endogenous production of 25-HC in macrophages, thereby regulating immune and antiviral functions (57–59). Therefore, it is plausible that hydrolysis of 25-HC ester may be involved in the regulation of the immune system by affecting these pathways.

Surprisingly, nonelicited peritoneal macrophages were highly sensitive to 25-HC even in the presence of *Nceh1* (supplementary Fig. 1). Conceivably, both the lower expression of *Nceh1* and the higher expression of *Acat1* render nonelicited macrophages susceptible to 25-HC-induced ER stress and apoptosis. In other words, the inflammatory state provoked by thioglycollate changes the property of macrophages making them more resistant to 25-HC as long as *Nceh1* is present. *Nceh1* appears to protect inflammatory

macrophages from oxysterol-induced apoptosis, thereby perpetuating inflammation into chronic phase, as is observed in atherosclerosis.

In conclusion, *Nceh1* plays a protective role in the oxysterol-induced apoptosis of macrophages. The accumulation of oxysterol esters in ER activates ER stress signaling. These findings should provide the basis for understanding the pathophysiology of the development of atherosclerosis and other diseases involving macrophage apoptosis. **FIG 7**

The authors thank Ms. Yukiko Hoshino and Mika Hayashi for technical assistance. The authors also thank Dr. Ikuyo Ichi at Ochanomizu University for preliminary experiments using GC/MS.

REFERENCES

- Weber, C., A. Zernecke, and P. Libby. 2008. The multifaceted contributions of leukocyte subsets to atherosclerosis: lessons from mouse models. *Nat. Rev. Immunol.* 8: 802–815.
- Okazaki, H., M. Igarashi, M. Nishi, M. Sekiya, M. Tajima, S. Takase, M. Takanashi, K. Ohta, Y. Tamura, S. Okazaki, et al. 2008.

- Identification of neutral cholesterol ester hydrolase, a key enzyme removing cholesterol from macrophages. *J. Biol. Chem.* **283**: 33357–33364.
3. Nomura, D. K., D. Leung, K. P. Chiang, G. B. Quistad, B. F. Cravatt, and J. E. Casida. 2005. A brain detoxifying enzyme for organophosphorus nerve poisons. *Proc. Natl. Acad. Sci. USA.* **102**: 6195–6200.
 4. Yeaman, S. J. 2004. Hormone-sensitive lipase—new roles for an old enzyme. *Biochem. J.* **379**: 11–22.
 5. Zhao, B., J. Song, W. N. Chow, R. W. St Clair, L. L. Rudel, and S. Ghosh. 2007. Macrophage-specific transgenic expression of cholesterol ester hydrolase significantly reduces atherosclerosis and lesion necrosis in Ldlr mice. *J. Clin. Invest.* **117**: 2983–2992.
 6. Sekiya, M., J. I. Osuga, M. Igarashi, H. Okazaki, and S. Ishibashi. 2011. The role of neutral cholesterol ester hydrolysis in macrophage foam cells. *J. Atheroscler. Thromb.* **18**: 359–364.
 7. Igarashi, M., J. I. Osuga, M. Isshiki, M. Sekiya, H. Okazaki, S. Takase, M. Takanashi, K. Ohta, M. Kumagai, M. Nishi, et al. 2009. Targeting of neutral cholesterol ester hydrolase to the endoplasmic reticulum via its N-terminal sequence. *J. Lipid Res.* **51**: 274–285.
 8. Chiang, K. P., S. Niessen, A. Saghatelian, and B. F. Cravatt. 2006. An enzyme that regulates ether lipid signaling pathways in cancer annotated by multidimensional profiling. *Chem. Biol.* **13**: 1041–1050.
 9. Sekiya, M., J. Osuga, S. Nagashima, T. Ohshiro, M. Igarashi, H. Okazaki, M. Takahashi, F. Tazoe, T. Wada, K. Ohta, et al. 2009. Ablation of neutral cholesterol ester hydrolase 1 accelerates atherosclerosis. *Cell Metab.* **10**: 219–228.
 10. Igarashi, M., J. Osuga, H. Uozaki, M. Sekiya, S. Nagashima, M. Takahashi, S. Takase, M. Takanashi, Y. Li, K. Ohta, et al. 2010. The critical role of neutral cholesterol ester hydrolase 1 in cholesterol removal from human macrophages. *Circ. Res.* **107**: 1387–1395.
 11. Li, A. C., and C. K. Glass. 2002. The macrophage foam cell as a target for therapeutic intervention. *Nat. Med.* **8**: 1235–1242.
 12. Harada, K., Z. Chen, S. Ishibashi, J. Osuga, H. Yagyu, K. Ohashi, N. Yahagi, F. Shionoiri, L. Sun, Y. Yazaki, and N. Yamada. 1997. Apoptotic cell death in atherosclerotic plaques of hyperlipidemic knockout mice. *Atherosclerosis.* **135**: 235–239.
 13. Seimon, T., and I. Tabas. 2009. Mechanisms and consequences of macrophage apoptosis in atherosclerosis. *J. Lipid Res.* **50(Suppl)**: S382–S387.
 14. Chisolm, G. M., G. Ma, K. C. Irwin, L. L. Martin, K. G. Gunderson, L. F. Linberg, D. W. Morel, and P. E. DiCorleto. 1994. 7 beta-hydroperoxycholest-5-en-3 beta-ol, a component of human atherosclerotic lesions, is the primary cytotoxin of oxidized human low density lipoprotein. *Proc. Natl. Acad. Sci. USA.* **91**: 11452–11456.
 15. Rusinól, A. E., L. Yang, D. Thewke, S. R. Panini, M. F. Kramer, and M. S. Sinensky. 2000. Isolation of a somatic cell mutant resistant to the induction of apoptosis by oxidized low density lipoprotein. *J. Biol. Chem.* **275**: 7296–7303.
 16. Panini, S. R., L. Yang, A. E. Rusinól, M. S. Sinensky, J. V. Bonventre, and C. C. Leslie. 2001. Arachidonate metabolism and the signaling pathway of induction of apoptosis by oxidized LDL/oxysterol. *J. Lipid Res.* **42**: 1678–1686.
 17. Rusinól, A. E., D. Thewke, J. Liu, N. Freeman, S. R. Panini, and M. S. Sinensky. 2004. AKT/protein kinase B regulation of BCL family members during oxysterol-induced apoptosis. *J. Biol. Chem.* **279**: 1392–1399.
 18. Freeman, N. E., A. E. Rusinól, M. Linton, D. L. Hachey, S. Fazio, M. S. Sinensky, and D. Thewke. 2005. Acyl-coenzyme A:cholesterol acyltransferase promotes oxidized LDL/oxysterol-induced apoptosis in macrophages. *J. Lipid Res.* **46**: 1933–1943.
 19. Kellner-Weibel, G., W. G. Jerome, D. M. Small, G. J. Warner, J. K. Stoltenborg, M. A. Kearney, M. H. Corjay, M. C. Phillips, and G. H. Rothblat. 1998. Effects of intracellular free cholesterol accumulation on macrophage viability: a model for foam cell death. *Arterioscler. Thromb. Vasc. Biol.* **18**: 423–431.
 20. Yao, P. M., and I. Tabas. 2000. Free cholesterol loading of macrophages induces apoptosis involving the fas pathway. *J. Biol. Chem.* **275**: 23807–23813.
 21. Devries-Seimon, T., Y. Li, P. M. Yao, E. Stone, Y. Wang, R. J. Davis, R. Flavell, and I. Tabas. 2005. Cholesterol-induced macrophage apoptosis requires ER stress pathways and engagement of the type A scavenger receptor. *J. Cell Biol.* **171**: 61–73.
 22. Yagyu, H., T. Kitamine, J. Osuga, R. Tozawa, Z. Chen, Y. Kaji, T. Oka, S. Perrey, Y. Tamura, K. Ohashi, et al. 2000. Absence of ACAT-1 attenuates atherosclerosis but causes dry eye and cutaneous xanthomatosis in mice with congenital hyperlipidemia. *J. Biol. Chem.* **275**: 21324–21330.
 23. Fazio, S., A. S. Major, L. L. Swift, L. A. Gleaves, M. Accad, M. F. Linton, and R. V. Farese, Jr. 2001. Increased atherosclerosis in LDL receptor-null mice lacking ACAT1 in macrophages. *J. Clin. Invest.* **107**: 163–171.
 24. Ikenoya, M., Y. Yoshinaka, H. Kobayashi, K. Kawamine, K. Shibuya, F. Sato, K. Sawanobori, T. Watanabe, and A. Miyazaki. 2007. A selective ACAT-1 inhibitor, K-604, suppresses fatty streak lesions in fat-fed hamsters without affecting plasma cholesterol levels. *Atherosclerosis.* **191**: 290–297.
 25. Takahashi, K., M. Kasai, M. Ohta, Y. Shoji, K. Kunishiro, M. Kanda, K. Kurahashi, and H. Shirahase. 2008. Novel indoline-based acyl-CoA:cholesterol acyltransferase inhibitor with antiperoxidative activity: improvement of physicochemical properties and biological activities by introduction of carboxylic acid. *J. Med. Chem.* **51**: 4823–4833.
 26. Omura, S., H. Tomoda, Y. K. Kim, and H. Nishida. 1993. Pyripyropenes, highly potent inhibitors of acyl-CoA:cholesterol acyltransferase produced by *Aspergillus fumigatus*. *J. Antibiot. (Tokyo).* **46**: 1168–1169.
 27. Ohshiro, T., D. Matsuda, K. Sakai, C. Degirolamo, H. Yagyu, L. L. Rudel, S. Omura, S. Ishibashi, and H. Tomoda. 2011. Pyripyropene A, an acyl-coenzyme A:cholesterol acyltransferase 2-selective inhibitor, attenuates hypercholesterolemia and atherosclerosis in murine models of hyperlipidemia. *Arterioscler. Thromb. Vasc. Biol.* **31**: 1108–1115.
 28. Okazaki, H., J. Osuga, K. Tsukamoto, N. Isoo, T. Kitamine, Y. Tamura, S. Tomita, M. Sekiya, N. Yahagi, Y. Iizuka, et al. 2002. Elimination of cholesterol ester from macrophage foam cells by adenovirus-mediated gene transfer of hormone-sensitive lipase. *J. Biol. Chem.* **277**: 31893–31899.
 29. Osuga, J., S. Ishibashi, T. Oka, H. Yagyu, R. Tozawa, A. Fujimoto, F. Shionoiri, N. Yahagi, F. B. Kraemer, O. Tsutsumi, and N. Yamada. 2000. Targeted disruption of hormone-sensitive lipase results in male sterility and adipocyte hypertrophy, but not in obesity. *Proc. Natl. Acad. Sci. USA.* **97**: 787–792.
 30. Sekiya, M., J. Osuga, H. Okazaki, N. Yahagi, K. Harada, W. J. Shen, Y. Tamura, S. Tomita, Y. Iizuka, K. Ohashi, et al. 2004. Absence of hormone-sensitive lipase inhibits obesity and adipogenesis in Lep ob/ob mice. *J. Biol. Chem.* **279**: 15084–15090.
 31. Harada, K., S. Ishibashi, T. Miyashita, J. Osuga, H. Yagyu, K. Ohashi, Y. Yazaki, and N. Yamada. 1997. Bcl-2 protein inhibits oxysterol-induced apoptosis through suppressing CPP32-mediated pathway. *FEBS Lett.* **411**: 63–66.
 32. Honda, A., K. Yamashita, T. Hara, T. Ikegami, T. Miyazaki, M. Shirai, G. Xu, M. Numazawa, and Y. Matsuzaki. 2009. Highly sensitive quantification of key regulatory oxysterols in biological samples by LC-ESI-MS/MS. *J. Lipid Res.* **50**: 350–357.
 33. Hosogai, N., A. Fukuhara, K. Oshima, Y. Miyata, S. Tanaka, K. Segawa, S. Furukawa, Y. Tochino, R. Komuro, M. Matsuda, and I. Shimomura. 2007. Adipose tissue hypoxia in obesity and its impact on adipocytokine dysregulation. *Diabetes.* **56**: 901–911.
 34. Schroepfer, G. J., Jr. 2000. Oxysterols: modulators of cholesterol metabolism and other processes. *Physiol. Rev.* **80**: 361–554.
 35. Chang, T. Y., C. C. Chang, N. Ohgami, and Y. Yamauchi. 2006. Cholesterol sensing, trafficking, and esterification. *Annu. Rev. Cell Dev. Biol.* **22**: 129–157.
 36. Sakashita, N., A. Miyazaki, C. C. Chang, T. Y. Chang, E. Kiyota, M. Satoh, Y. Komohara, P. M. Morganeli, S. Horiuchi, and M. Takeya. 2003. Acyl-coenzyme A:cholesterol acyltransferase 2 (ACAT2) is induced in monocyte-derived macrophages: in vivo and in vitro studies. *Lab. Invest.* **83**: 1569–1581.
 37. Ron, D., and P. Walter. 2007. Signal integration in the endoplasmic reticulum unfolded protein response. *Nat. Rev. Mol. Cell Biol.* **8**: 519–529.
 38. Kim, I., W. Xu, and J. C. Reed. 2008. Cell death and endoplasmic reticulum stress: disease relevance and therapeutic opportunities. *Nat. Rev. Drug Discov.* **7**: 1013–1030.
 39. Radhakrishnan, A., Y. Ikeda, H. J. Kwon, M. S. Brown, and J. L. Goldstein. 2007. Sterol-regulated transport of SREBPs from endoplasmic reticulum to Golgi: oxysterols block transport by binding to Insig. *Proc. Natl. Acad. Sci. USA.* **104**: 6511–6518.
 40. Gargalovic, P., and L. Dory. 2003. Cellular apoptosis is associated with increased cavolin-1 expression in macrophages. *J. Lipid Res.* **44**: 1622–1632.
 41. Peet, D. J., B. A. Janowski, and D. J. Mangelsdorf. 1998. The LXRs: a new class of oxysterol receptors. *Curr. Opin. Genet. Dev.* **8**: 571–575.

42. Brown, A. J., and W. Jessup. 1999. Oxysterols and atherosclerosis. *Atherosclerosis*. **142**: 1–28.
43. Brown, M. S., S. E. Dana, and J. L. Goldstein. 1975. Cholesterol ester formation in cultured human fibroblasts. Stimulation by oxygenated sterols. *J. Biol. Chem.* **250**: 4025–4027.
44. Peng, S. K., P. Tham, C. B. Taylor, and B. Mikkelsen. 1979. Cytotoxicity of oxidation derivatives of cholesterol on cultured aortic smooth muscle cells and their effect on cholesterol biosynthesis. *Am. J. Clin. Nutr.* **32**: 1033–1042.
45. Chang, T. Y., and J. S. Limanek. 1980. Regulation of cytosolic acetoacetyl coenzyme A thiolase, 3-hydroxy-3-methylglutaryl coenzyme A synthase, 3-hydroxy-3-methylglutaryl coenzyme A reductase, and mevalonate kinase by low density lipoprotein and by 25-hydroxycholesterol in Chinese hamster ovary cells. *J. Biol. Chem.* **255**: 7787–7795.
46. Yang, J., R. Sato, J. L. Goldstein, and M. S. Brown. 1994. Sterol-resistant transcription in CHO cells caused by gene rearrangement that truncates SREBP-2. *Genes Dev.* **8**: 1910–1919.
47. Yang, J., M. S. Brown, Y. K. Ho, and J. L. Goldstein. 1995. Three different rearrangements in a single intron truncate sterol regulatory element binding protein-2 and produce sterol-resistant phenotype in three cell lines. Role of introns in protein evolution. *J. Biol. Chem.* **270**: 12152–12161.
48. Hua, X., A. Nohturfft, J. L. Goldstein, and M. S. Brown. 1996. Sterol resistance in CHO cells traced to point mutation in SREBP cleavage-activating protein. *Cell*. **87**: 415–426.
49. Cadigan, K. M., J. G. Heider, and T. Y. Chang. 1988. Isolation and characterization of Chinese hamster ovary cell mutants deficient in acyl-coenzyme A:cholesterol acyltransferase activity. *J. Biol. Chem.* **263**: 274–282.
50. Metherall, J. E., N. D. Ridgway, P. A. Dawson, J. L. Goldstein, and M. S. Brown. 1991. A 25-hydroxycholesterol-resistant cell line deficient in acyl-CoA: cholesterol acyltransferase. *J. Biol. Chem.* **266**: 12734–12740.
51. Cheng, D., C. C. Chang, X. Qu, and T. Y. Chang. 1995. Activation of acyl-coenzyme A:cholesterol acyltransferase by cholesterol or by oxysterol in a cell-free system. *J. Biol. Chem.* **270**: 685–695.
52. Lichtenstein, A. H., and P. Brecher. 1983. Esterification of cholesterol and 25-hydroxycholesterol by rat liver microsomes. *Biochim. Biophys. Acta.* **751**: 340–348.
53. Shibata, N., A. F. Carlin, N. J. Spann, K. Saijo, C. S. Morello, J. G. McDonald, C. E. Romanoski, M. R. Maurya, M. U. Kaikkonen, M. T. Lam, et al. 2013. 25-Hydroxycholesterol activates the integrated stress response to reprogram transcription and translation in macrophages. *J. Biol. Chem.* **288**: 35812–35823.
54. Bansal, N., A. Houle, and G. Melnykovich. 1991. Apoptosis: mode of cell death induced in T cell leukemia lines by dexamethasone and other agents. *FASEB J.* **5**: 211–216.
55. Baldán, A., L. Pei, R. Lee, P. Tarr, R. K. Tangirala, M. M. Weinstein, J. Frank, A. C. Li, P. Tontonoz, and P. A. Edwards. 2006. Impaired development of atherosclerosis in hyperlipidemic Ldlr^{-/-} and ApoE^{-/-} mice transplanted with Abcg1^{-/-} bone marrow. *Arterioscler. Thromb. Vasc. Biol.* **26**: 2301–2307.
56. Infante, R. E., A. Radhakrishnan, L. Abi-Mosleh, L. N. Kinch, M. L. Wang, N. V. Grishin, J. L. Goldstein, and M. S. Brown. 2008. Purified NPC1 protein: II. Localization of sterol binding to a 240-amino acid soluble luminal loop. *J. Biol. Chem.* **283**: 1064–1075.
57. Bauman, D. R., A. D. Bitmansour, J. G. McDonald, B. M. Thompson, G. Liang, and D. W. Russell. 2009. 25-Hydroxycholesterol secreted by macrophages in response to Toll-like receptor activation suppresses immunoglobulin A production. *Proc. Natl. Acad. Sci. USA.* **106**: 16764–16769.
58. Liu, S. Y., R. Aliyari, K. Chikere, G. Li, M. D. Marsden, J. K. Smith, O. Pernet, H. Guo, R. Nusbaum, J. A. Zack, et al. 2013. Interferon-inducible cholesterol-25-hydroxylase broadly inhibits viral entry by production of 25-hydroxycholesterol. *Immunity*. **38**: 92–105.
59. Blanc, M., W. Y. Hsieh, K. A. Robertson, K. A. Kropp, T. Forster, G. Shui, P. Lacaze, S. Watterson, S. J. Griffiths, N. J. Spann, et al. 2013. The transcription factor STAT-1 couples macrophage synthesis of 25-hydroxycholesterol to the interferon antiviral response. *Immunity*. **38**: 106–118.